Arabian Journal of Chemistry (2015) 8, 732–741

King Saud University

Arabian Journal of Chemistry

www.ksu.edu.sa
www.sciencedirect.com

ORIGINAL ARTICLE

Green synthesis of silver nanoparticles from marigold flower and its synergistic antimicrobial potential

Hemali Padalia, Pooja Moteriya, Sumitra Chanda *

Phytochemical, Pharmacological and Microbiological Laboratory, Department of Biosciences, Saurashtra University, Rajkot 360 005, Gujarat, India

Received 9 June 2014; accepted 3 November 2014
Available online 8 November 2014

KEYWORDS

Tagetes erecta;
Marigold;
Silver nanoparticles;
Spectral analysis;
Antimicrobial activity

Abstract In the present study, silver nanoparticles were synthesized using flower broth of *Tagetes erecta* as reductant by a simple and eco-friendly route. The aqueous silver ions when exposed to flower broth were reduced and resulted in green synthesis of silver nanoparticles. The silver nanoparticles were characterized by UV–visible spectroscopy, zeta potential, Fourier transform infra-red spectroscopy (FTIR), X-ray diffraction, Transmission electron microscopy (TEM) analysis, Energy dispersive X-ray analysis (EDX) and selected area electron diffraction (SAED) pattern. UV–visible spectrum of synthesized silver nanoparticles showed maximum peak at 430 nm. TEM analysis revealed that the particles were spherical, hexagonal and irregular in shape and size ranging from 10 to 90 nm and Energy dispersive X-ray (EDX) spectrum confirmed the presence of silver metal. Synergistic antimicrobial potential of silver nanoparticles was evaluated with various commercial antibiotics against Gram positive (*Staphylococcus aureus* and *Bacillus cereus*), Gram negative (*Escherichia coli* and *Pseudomonas aeruginosa*) bacteria and fungi (*Candida glabrata*, *Candida albicans*, *Cryptococcae neoformans*). The antifungal activity of AgNPs with antibiotics was better than antibiotics alone against the tested fungal strains and Gram negative bacteria, thus signification of the present study is in production of biomedical products.

1. Introduction

The field of nanotechnology is one of the most active areas of research in current material science. The synthesis and characterization of noble metal nanoparticles such as silver, gold and platinum is an emerging field of research due to their important applications in the fields of biotechnology, bioengineering, textile engineering, water treatment, metal-based consumer products and other areas, electronic, magnetic, optoelectron-

* Corresponding author.
E-mail address: svchanda@gmail.com (S. Chanda).
Peer review under responsibility of King Saud University.

Production and hosting by Elsevier

http://dx.doi.org/10.1016/j.arabjc.2014.11.015
1878-5352

ics, and information storage (Rafiuddin, 2013). It has been reported that since ancient times silver metal is known to have antimicrobial activities (Pal et al., 2007) and silver nanoparticles (AgNPs) are of particular interest due to their peculiar properties and wide applications. Silver nanoparticles are used to treat infections in open wounds, chronic ulcers (Parashar et al., 2009) and in textiles, home water purification systems, medical devices, cosmetics, electronics, and household appliances (Wijnhoven et al., 2009), catalysis, biosensing, imaging, drug delivery, nanodevice fabrication and in medicine (Lee and El-Sayed, 2006; Nair and Laurencin, 2007; Jain et al., 2008), treatment of brucellosis (Alizadeh et al., 2013), anti-inflammatory (Wong et al., 2009), mosquito larvicidal (Rawani et al., 2013), etc.

Recently, resistance to commercially available antimicrobial agents by pathogenic bacteria and fungi is increasing at an alarming rate and has become a global threat. Drug resistance is one of the most serious and widespread problems in all developing countries (Stevanovic et al., 2012). Day by day treating bacterial infection is increasingly complicated because of the ability of the pathogens to develop resistance to available antimicrobial agents and existing antibiotics. Resistant pathogens may spread and become broader infection control problems within hospitals and communities as well. Resistant bacteria like *Staphylococci*, *Enterococci*, *Klebsiella pneumoniae* and *Pseudomonas* spp. are becoming more and more common (Tenover, 2006). To circumvent this, novel methods or novel strategies are required. The successful approach was the use of natural antimicrobials, combination or synergistic therapy and more recently use of metal nanoparticles.

Numerous methodologies are invented to synthesize noble metal nanoparticles of particular shape and size depending on specific requirements, because properties of metallic nanoparticles dependent on size and shape are of interest for applications ranging from catalysts and sensing to optics, antibacterial activity and data storage (Li et al., 2010). The surface to volume ratio of nanoparticles is inversely proportional to their size. The biological effectiveness of nanoparticles can increase proportionately with an increase in the specific surface area due to the increase in their surface energy and catalytic reactivity. Many methods have been used for the synthesis of silver nanoparticles, like chemical and photochemical reduction (Chen et al., 2001; Frattini et al., 2005) electrochemical techniques (Khaydarov et al., 2009) and radiolysis methods (Henglein, 1993).

However, in most of the methods hazardous chemicals and low material conversions and high energy requirements are used for the preparation of nanoparticles (Sathyavathi et al., 2010; Bar et al., 2009; Venkatesham et al., 2014). So, there is a need to develop high-yield, low cost, non-toxic and environmentally friendly procedures. In such a situation, biological approach appears to be very appropriate. Natural material like plants, bacteria, fungi, yeast, are used for synthesis of silver nanoparticles (Rangnekar et al., 2007; Ahmad et al., 2013; Sumana et al., 2013; Kotakadi et al., 2014; Vidhu and Philip, 2014).

Tagetes erecta (Marigold) is an ornamental plant belonging to the family Asteraceae. Flowers of this plant are used in garlands for social and religious purposes in most of the countries. It is native to Mexico and widely distributed in South East Asia including Bangladesh and India. The flowers are bright yellow, brownish-yellow or orange. Different parts of this plant including flower is used in folk medicine. In has been used for skin complaints, wounds and burns, conjunctivitis and poor eyesight, menstrual irregularities, varicose veins, hemorrhoids, duodenal ulcers, etc (Wichtl, 1994; Krishnamurthy et al., 2012). The flowers are especially employed to cure eye diseases, colds, conjunctivitis, coughs, ulcer, bleeding piles and to purify blood (Kirtikar and Basu, 1994; Manjunath, 1969; Ghani, 2003). Repellent and biocide activities of essential oils of *T. erecta* against mosquito species have been reported (Singer, 1987; Wells et al., 1992). Antimicrobial activity of gold nanoparticles of flower extract is reported by Krishnamurthy et al. (2012).

In the present work, an attempt has been made to synthesize silver nanoparticles using aqueous flower extract of *T. erecta* (Fig. 1A). The characterization was done using several spectral analyses. The synthesized silver nanoparticles were evaluated for their synergistic antimicrobial activity.

2. Materials and method

2.1. Chemicals

Fresh flowers of *T. erecta* were purchased from the local market of Rajkot Gujarat, India. All the chemicals were obtained from Hi Media Laboratories and Sisco Research Laboratories Pvt. Limited, Mumbai, India. Ultra purified water was used for experiment.

2.2. Preparation of the extract for synthesis of silver nanoparticles

Fresh flowers were thoroughly washed with tap water, followed by double distilled water and cut into small pieces. 5 g of cut flowers was boiled for 10 min in 100 ml ultra pure water and filtered through Whatmann No. 1 filter paper. The filtered *T. erecta* extract was used for the synthesis of silver nanoparticles.

2.3. Preparation of crude extract

The dried powder of the marigold flower was extracted by cold percolation method. The powder was first defatted with hex-

Figure 1A *Tagetes erecta* plant.

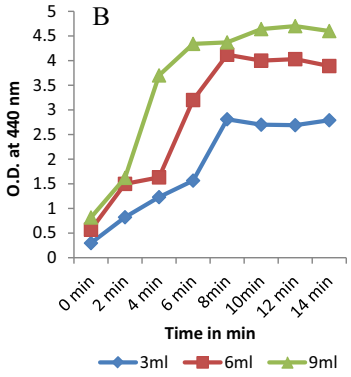

Figure 1B Effect of extract amount.

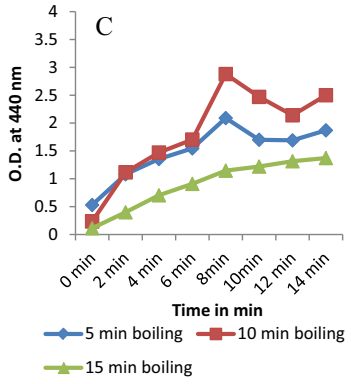

Figure 1C Effect of boiling time.

ane and then extracted in acetone as described earlier (Parekh and Chanda, 2007).

2.4. Synthesis of silver nanoparticles

Aqueous solution (1 mM) of silver nitrate ($AgNO_3$) was prepared and used for the synthesis of silver nanoparticles. 6 ml of extract was added to 40 ml of 1 mM $AgNO_3$ solution for the reduction of Ag^+ ions. The synthesis of silver nanoparticles was carried out at room temperature (25 °C ± 2 °C) for 24 h in dark. The silver nanoparticle solution thus obtained was purified by repeated centrifugation at 10,000 rpm for 10 min followed by redispersion of the pellet of silver nanoparticles into acetone. After air drying of the purified silver particles they were stored at 4 °C for further analysis.

2.5. Standardization

For efficient synthesis of silver nanoparticles, effect of boiling time and effect of extract amount to be added to 1 Mm $AgNO_3$ solution were varied and the best one was selected. The formation of AgNPs was monitored as a function of time of reaction on a spectrophotometer by taking O.D. at 440 nm at an interval of 2 min.

2.6. Characterization of the synthesized silver nanoparticles

UV–Vis spectra of synthesized nanoparticles were monitored as a function of time of reaction on a spectrophotometer (Shimadzu UV-1601) in 400–700 nm range operated at a resolution of 10 nm. The FTIR (Fourier transform infra-red spectroscopy) was recorded in the range of 400–4000 cm^{-1} Nicolet IS10 (Thermo Scientific, USA). Various modes of vibrations were identified and assigned to determine the different functional groups present in the *T. erecta* extract. The zeta potential measurement was performed using a Microtra (Zetatra Instruments). The structure and composition of synthesized silver nanoparticles was analyzed by XRD (X-ray diffraction). The formation of Ag nanoparticles was determined by an X'Pert Pro X-ray diffractometer (PAN analytical BV) operated at a voltage of 40 kV and a current of 30 mA with Cu Kα radiation in θ–2θ configurations. The crystallite domain size was calculated from the width of the XRD peaks, assuming that they are free from non-uniform strains, using the Scherrer formula. $D = 0.94\lambda/\beta \mathrm{Cos}\theta$ where D is the average crystallite domain size perpendicular to the reflecting planes, λ is the X-ray wavelength, β is the full width at half maximum (FWHM), and θ is the diffraction angle. TEM (Transmission electron microscopy) analysis was done to visualize the shape as well as to measure the diameter of the bio-synthesized silver nanoparticles. The sample was dispersed in double distilled water. A drop of thin dispersion was placed on a "staining

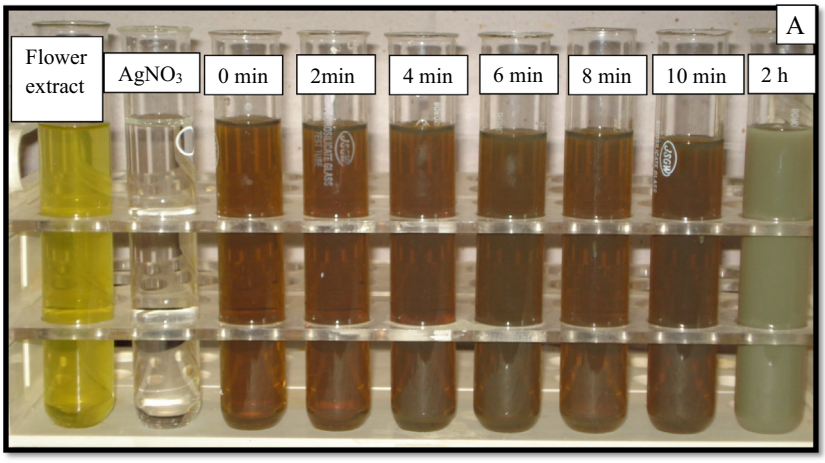

Figure 2A Color change in the reaction mixture within 10 min.

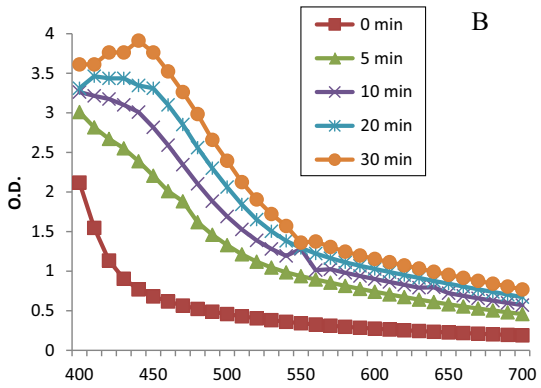

Figure 2B UV–visible spectrum of biosynthesized TE–AgNPs at different time intervals, showed peak at 430 nm.

mat''. Carbon coated copper grid was inserted into the drop with the coated side upwards. After about 10 min, the grid was removed and air dried. Then screened in JEOL JEM 2100 Transmission Electron Microscope.

2.7. Antimicrobial activity

The antimicrobial activity of crude acetone extract and synthesized *T. erecta* AgNPs with 15 commercial antibiotics and antibiotics alone was determined against 2 Gram positive bacteria (*Staphylococcus aureus* and *Bacillus cereus*) and 2 Gram negative bacteria (*Escherichia coli* and *Pseudomonas aeruginosa*) and 3 fungal (*Candida albicans*, *Candida glabrata*, *Cryptococcae neoformans*) strains, by using agar disc diffusion method (Rakholiya and Chanda, 2012).

3. Results

3.1. Standardization

There was a difference in the formation of AgNPs by 5 and 10 min and 15 min boiling time. Maximum AgNP formation occurred at 10 min boiling time (Fig. 1B). Hence, 10 min boiling time was finalized for the preparation of the flower extract. On adding 6 ml of the extract, AgNP formation was consider-

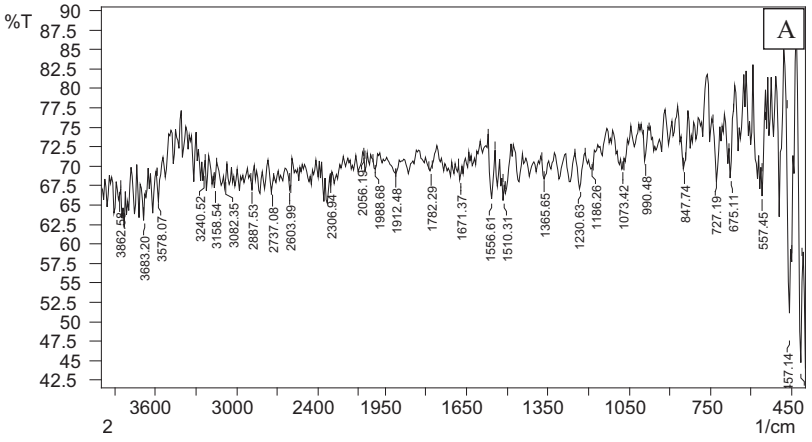

Figure 3A FTIR spectrum of biosynthesized AgNPs.

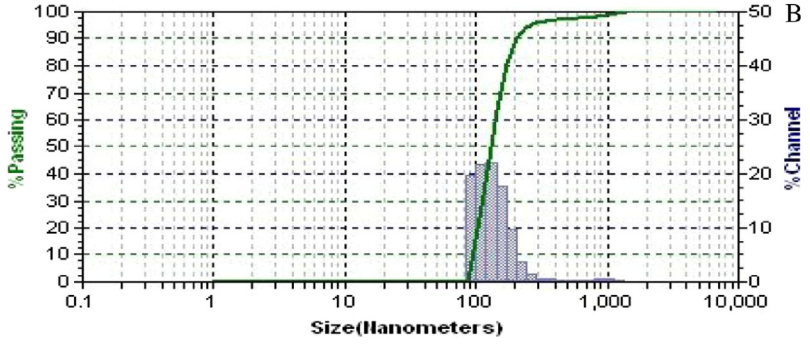

Mobility	-0.90μ/s/v/cm
Zeta potential	-27.63 mv
Charge	-0.05685 fc
Polarity	Negative
conductivity	55μs/cm

Figure 3B Zeta potential measurements of biosynthesized AgNPs.

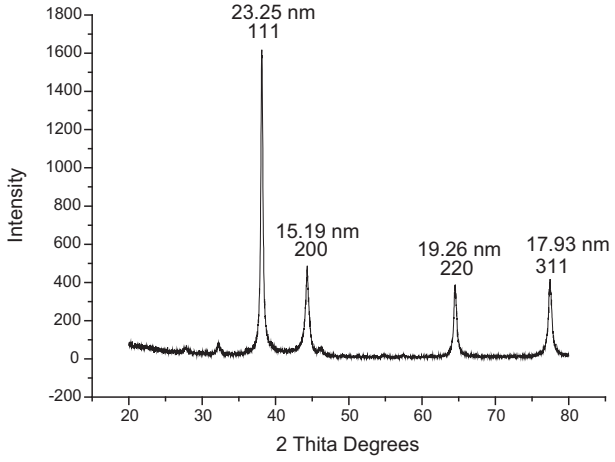

Figure 4 XRD spectrum of biosynthesized *Tagetes erecta* flower AgNPs.

ably more than on addition of 3 ml but on adding 9 ml of extract, formation of AgNPs was not very much different (Fig. 1C). Hence, 6 ml extract was finalized for the synthesis of AgNPs.

3.2. Characterization

On adding light yellow color flower extract to color less silver nitrate solution, formation of AgNPs occurred and they exhibited a color change to surface plasmon resonance. The intensity of color was directly proportional to the formation of AgNPs. The color change was very rapid and as soon as the two solutions were mixed, the solution turned brown and within 10 min, it turned to dark brown and by 2 h the solution turned black (Fig. 2A). The UV–vis spectra recorded from the flower extract of *T. erecta* reaction at different time intervals is presented in Fig. 2B. The spectrum showed maximum absorption band at 430 nm. The absorbance steadily increased in

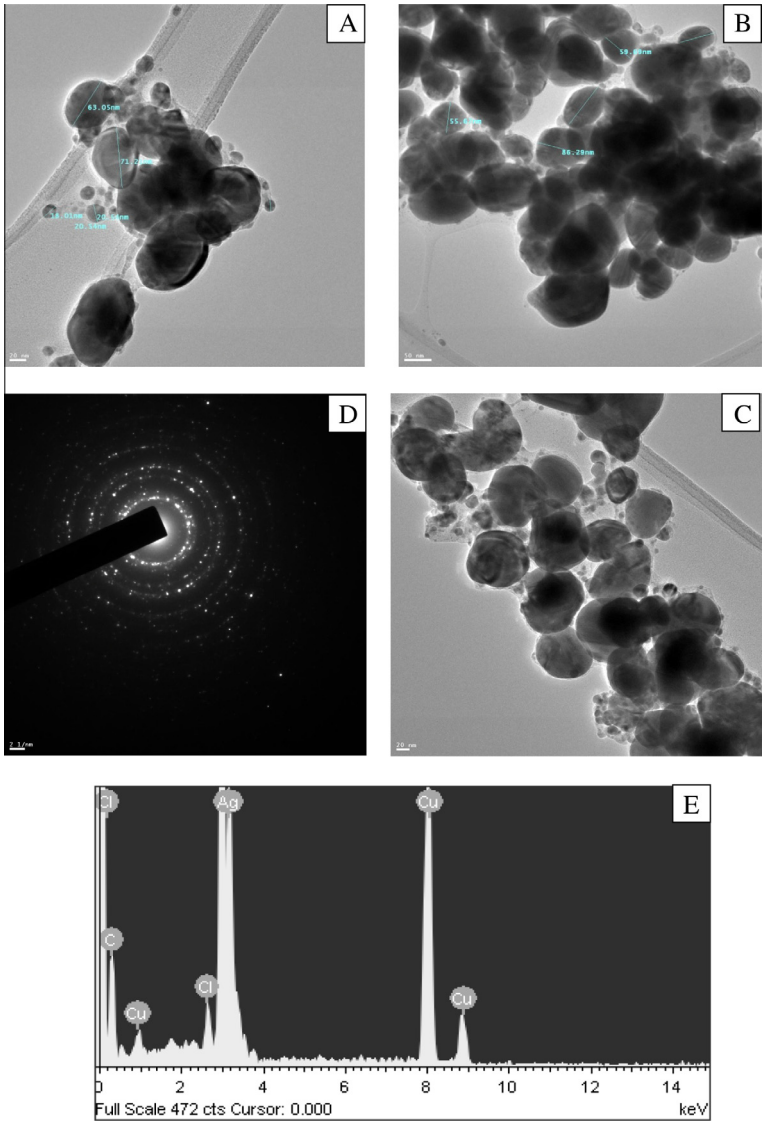

Figure 5 TEM images (A, B, C) of Ag nanoparticles in low and high magnification, (D) SAED patterns of the silver nanoparticles, (E) EDX spectrum showed higher percentage of silver signal.

intensity as a function of reaction time. Stability of AgNPs is determined by zeta potential measurement. Zeta potential value ±30 mv is considered as stable nano suspension. The zeta potential of *T. erecta* flower AgNPs was −27.63 mV (Fig. 3B). This suggested that the surface of the nanoparticles was negatively charged that dispersed in the medium. FTIR analysis was done to identify the possible bio-reducing biomolecules in the flower extract. Fig. 3A shows the FTIR spectra of aqueous silver nanoparticles prepared from the *T. erecta* flower extract. The band at 3740.10 cm^{-1} corresponds to N—H amide stretching. The peak at 727.19 cm^{-1} corresponds to C—H stretching strong aromatic monosubstituted benzene. The assignment at 793.73 cm^{-1} corresponds to C—Cl stretching alkyl halides and 693.43 cm^{-1} corresponds to C—H stretching strong vinyl disubstituted alkenes. X-ray diffraction (XRD) patterns of silver nanoparticles indicate that the structure of silver nanoparticles is face-centered cubic (fcc) (Fig. 4). In addition, the diffraction peaks at 2Φ values of 23.25, 15.19, 19.20, 17.93 could be attributed to (111), (200), (220), (311) Braggs reflection respectively. The lattice constant calculated from this pattern was 4.0865 A. The obtained value was according to the joint committee on powder diffraction standards (JCPDS) file No. 04-0783.

3.3. TEM analysis

The TEM image of the AgNPs is depicted in Fig. 5. The size was in the range of 10–90 nm; the average size of the nanoparticles was found to be 46.11 nm (Fig. 5A, B). The shape of the nanoparticles was spherical, hexagonal and irregular in shape with moderate variation in size (Fig. 5C). In order to verify the crystalline nature of the nanoparticles the selected area electron diffraction (SAED) patterns were obtained for the sample containing 1 mM of $AgNO_3$, for different regions and particles, as shown in Fig. 5D. The ring like diffraction pattern in SAED image indicates that particles are purely crystalline in nature and could be indexed on the basis of the face centered cubic silver structure. The bright ring arise due to reflection from (111), (200), (220), and (311) planes of fcc silver which is supported by XRD results. The results of EDX analysis are shown in Fig. 5E. Presence of elemental silver can be seen in the graph by EDX analysis in support of XRD results.

Table 1 Phytochemical test of *T. erecta* flower powder.

Test	Result
Flavanoids	+ + + +
Tannins	+ + +
Phlobatannins	–
Triterpenes	+ + +
Steroids	–
Saponins	–
Cardiac glycoside	+ + +
Meyer's	–
Dragondroff	+ + + +
Wagners	+ + +
Legal's	–

Table 2A Synergistic activity of AgNPs of *T. erecta* flower with different standard antibiotics against Gram negative and Gram positive bacteria.

Anti biotic	*Escherichia coli* (NCIM NO 2931)			*Pseudomonas aeruginosa* (ATCC NO 27853)			*Bacillus cereus* (ATCC NO 11778)			*Staphylococcus aureus* (ATCC NO 29737)		
	Anti biotic (A) (mm)	Anti biotic + AgNPs (B) (mm)	Increase In fold area	Anti biotic (A)(mm)	Anti biotic + AgNPs (B) (mm)	Increase In Fold area	Anti biotic (A) (mm)	Anti biotic + AgNPs (B) (mm)	Increase In fold area	Anti biotic (A) (mm)	Anti biotic + AgNPs (B) (mm)	Increase In fold area
AMP	9	10	0.23	23	24.5	0.13	–	–	–	34	36	0.12
PB^{100}	9	10	0.23	13.5	14.2	0.11	11	9	0	9	10	0.23
Gen^{10}	13.5	17	0.59	22	22	0	19.5	20.5	0.11	16	17.5	0.2
C^{30}	25.5	26.5	0.08	14	15.5	0.23	34	34	0	24	24	0
P^{10}	–	–	–	14	14.7	0.1	–	–	–	33	35	0.12
Ak^{10}	17.5	22.5	0.65	24.5	25.5	0.08	22	23.5	0.14	17	16	0
TE^{30}	22	26	0.4	26.5	31.5	0.41	27.5	27.5	0	28	28	0
CEP^{30}	11.5	11.5	0	11	13	0.4	13	13	0	37.5	38	0.03
AMC^{10}	9	9.5	0.11	20.5	22.5	0.2	–	–	–	31.5	32	0.02
CFP^{30}	9	11	0.49	34	34	0	13.5	14.5	0.01	24	23	0
CC^{10}	12	15.5	0.67	–	–	–	14	16.5	0.39	11.5	14.5	0.59

AMP – Ampicillin, PB^{100} – Polymyxin, Gen^{10} – Gentamicin, C^{30} – Chloramphenicol, P^{10} – Penicilli-G, AK^{10} – Amikacin, TE^{30} – Tetracycline, CEP^{30} – Cephalothin, AMC^{10} – Amoxyclav, CFP^{30} – Cefpirome, CC^{10} – Clotrimazole.
Mean surface area of the inhibition zone was calculated for each from the mean diameter.
Increase in fold area was calculated as $(B^2 - A^2)/A^2$, where A and B are the inhibition zones for Antibiotics and Antibiotics + AgNPs, respectively.

3.4. Antimicrobial activity

Out of 11 antibiotics tested, synergistic activity or increase in fold area of antibiotics plus acetone extract was against only one antibiotic i.e. CC^{10} against *B. cereus*. On the other hand, antibiotics plus AgNPs showed synergistic activity with three antibiotics, maximum being against CC^{10}. *S. aureus* was inhibited more than *B. cereus*, both with antibiotics plus acetone extract or antibiotics plus AgNPs (Tables 2A and 2B). Increase in fold area was more with acetone extract than with AgNPs. Antibiotics and acetone extract showed more activity against PB^{100} (1.8) followed by AMP (0.53) (Table 2B) while antibiotics and AgNPs showed more activity against CC^{10} (0.59) (Table 2A).

The antibacterial activity against *E. coli* and *P. aeruginosa* was definitely better than Gram positive bacteria. In spite of possessing much tougher cell wall, these bacteria were more inhibited both by antibiotics plus acetone extract and antibiotics plus AgNPs (Tables 2A and 2B). *E. coli* was inhibited by almost 7–8 antibiotics when antibiotics plus AgNPs were used or acetone extract with antibiotics was used, while *P. aeruginosa* was inhibited by 7 antibiotics when antibiotics plus AgNPs were used but when acetone extract plus antibiotics was used the activity was only against 4 antibiotics. Maximum increase in fold area was again against CC^{10} (0.67) by *E. coli* while *P. aeruginosa* did not show any activity against CC^{10}.

The antifungal activity was done with 4 antibiotics against 3 fungal strains; antibiotics plus AgNPs showed activity with all the 4 antibiotics against all the 3 fungal strains and maximum activity as evidenced by maximum increase in fold area was against *C. albicans* against KT^{30} followed by *C. neoformans* against KT^{39} (Table 3A). When the activity of antibiotics plus acetone extract is evaluated, it was observed that activity was shown only against *C. albicans* and maximum activity was again with KT^{30} (Table 3B). Antibiotics and acetone extract could not inhibit *C. neoformans* or *C. glabrata*.

4. Discussion

The different parts of plant extracts are ecofriendly, economical and safe for the synthesis of nanoparticles. Use of flower extract for synthesis of nanoparticles has an added advantage of environmental friendly. Flowers are normally thrown away into the environment, so evaluating therapeutic value of discarded material is a novel idea. In the present study, an attempt was made to synthesize silver nanoparticles from *T. erecta* flower extract. For synthesis of silver nanoparticles standardization was done in respect to addition of extract amount and boiling time for the preparation of plant extract. Optimization of these two parameters was essential as both had a profound effect on the formation of silver nanoparticles. Zayed et al. (2012) also reported effect of extract amount on AgNPs formation.

The colorless solution turned brown indicating the nanoparticle formation of silver. The characteristic brown color of silver provided a convenient spectroscopic signature to indicate nanoparticles formation. The formation of AgNPs occurs from few minutes to hours as reported for other plant extracts (Chanda, 2014). UV-spectra revealed maximum absorption peak at 430 nm and the intensity of absorption increased with time. The increase in intensity could be due to the increasing

Table 2B Synergistic activity of acetone extract of *T. erecta* flower with different standard antibiotics against Gram negative and Gram positive bacteria.

Anti biotic	*Escherichia coli* (NCIM NO 2931)			*Pseudomonas aeruginosa* (ATCC NO 27853)			*Bacillus cereus* (ATCC NO 11778)			*Staphylococcus aureus* (ATCC NO 29737)		
	Anti biotic (A) (mm)	Anti biotic + Acetone extracts (B) (mm)	Increase In fold area	Anti biotic (A) (mm)	Anti biotic + Acetone extracts (B) (mm)	Increase In Fold area	Antibiotic (A) (mm)	Anti biotic + Acetone extracts (B) (mm)	Increase In fold area	Anti biotic (A) (mm)	Anti biotic + Acetone extracts (B) (mm)	Increase In fold area
AMP	9	10	0.23	23	23.5	0.04	–	–	–	34	42	0.53
PB^{100}	9	10	0.23	13.5	14	0.08	11	10	0	9	15	1.8
Gen^{10}	13.5	17	0.59	22	21	0	19.5	17	0	16	16	0
C^{30}	25.5	22.5	0	14	16	0.30	34	33.5	0	24	27	0.23
P^{10}	–	–	–	14	–	0	–	–	–	33	33	0
Ak^{10}	17.5	21	0.44	24.5	25	0.04	22	21	0	17	16	0
TE^{30}	22	26	0.40	26.5	31	0.37	27.5	26	0	28	33	0.39
CEP^{30}	11.5	11	0	11	13	0.40	13	12	0	37.5	40	0.14
AMC^{10}	9	9	0	20.5	22.5	0.21	–	–	–	31.5	35	0.23
CFP^{30}	9	11	0.50	34	33	0	13.5	12	0	24	22	0
CC^{10}	12	15	0.57	–	–	–	14	15	0.15	11.5	14	0.49

AMP – Ampicillin, PB^{100} – Polymyxin, Gen^{10} – Gentamicin, C^{30} – Chloramphenicol, P^{10} – Penicilli-G, AK^{10} – Amikacin, TE^{30} – Tetracycline, CEP^{30} – Cephalothin, AMC^{10} – Amoxyclav, CFP^{30} – Cefpirome, CC^{10} – Clotrimazole.

Mean surface area of the inhibition zone was calculated for each from the mean diameter.

Increase in fold area was calculated as $(B^2 - A^2)/A^2$, where A and B are the inhibition zones for Antibiotics and Antibiotics + Acetone extracts, respectively.

Table 3A Synergistic activity of AgNPs of *T. erecta* flower with different standard antibiotics against fungi.

Anti biotic	*Candida glabrata* (NCIM NO 3448)			*Candida albicans* (NCIM NO 3102)			*Cryptococcae neoformans* (NCIM NO 3542)		
	Anti biotic (A) (mm)	Anti biotic + AgNPs (B) (mm)	Increase in fold area	Anti biotic (A) (mm)	Anti biotic + AgNPs(B) (mm)	Increase in fold area	Anti biotic (A) (mm)	Anti biotic + AgNPs(B) (mm)	Increase in fold area
NS^{100}	29	32	0.22	17	21	0.52	23.5	25	0.13
KT^{30}	24.5	29	0.40	15	19.5	0.70	15.5	19.5	0.58
FLC^{10}	21.5	26	0.46	20.5	21	0.05	13.5	14.7	0.19
AP^{100}	15	17	0.28	10.5	12	0.31	12	13	0.17

NS^{100} – Nystatin, KT^{30} – Ketoconazole, FLC^{10} – Fluconazole, AP^{10} – Ampotericin.
Mean surface area of the inhibition zone was calculated for each from the mean diameter.
Increase in fold area was calculated as $(B^2 - A^2)\ /A^2$, where A and B are the inhibition zones for Antibiotics and Antibiotics + AgNPs, respectively.

Table 3B Synergistic activity of acetone extract of *T. erecta* flower with different standard antibiotics against fungi.

Anti biotic	*Candida glabrata* (NCIM NO 3448)			*Candida albicans* (NCIM NO 3102)			*Cryptococcae neoformans* (NCIM NO 3542)		
	Antibiotic (A) (mm)	Anti biotic + Acetone extracts (B) (mm)	Increase in fold area	Anti Biotic (A) (mm)	Anti biotic + Acetone extracts (B) (mm)	Increase in fold area	Anti biotic (A) (mm)	Anti biotic + Acetone extracts (B) (mm)	Increase in fold area
NS^{100}	29	28	0	17	26	0.53	23.5	23	0
KT^{30}	24.5	17	0	15	24	1.56	15.5	12	0
FLC^{10}	21.5	18	0	20.5	17	0	13.5	13	0
AP^{100}	15	12	0	10.5	13	0.53	12	13	0.17

NS^{100} – Nystatin, KT^{30} – Ketoconazole, FLC^{10} – Fluconazole, AP^{10} – Ampotericin.
Mean surface area of the inhibition zone was calculated for each from the mean diameter.
Increase in fold area was calculated as $(B^2 - A^2)\ /A^2$, where A and B are the inhibition zones for Antibiotics and Antibiotics + Acetone extracts, respectively.

number of nanoparticles formed as a result of reduction of silver ions present in the aqueous solution with the help of phytoconstituents present in *T. erecta* flower extract. Similar results were reported by Pant et al. (2012) and Roopan et al. (2013).

The zeta potential of *T. erecta* flower AgNPs was −27.63 mv. According to Gengana et al. (2013) a zeta potential higher than 30 mV or lesser than −30 mv is indicative of a stable system. The negative charge on the surface of the synthesized AgNPs can cause strong repulsive force among particles which may prevent from aggregation. Hence, it can be concluded that the synthesized nanoparticles are fairly stable. The secondary metabolites like alkaloids, flavonoids, tannins and cardiac glycoside present in the flower extract may be responsible for stabilizing the synthesized nanoparticles (Table 1) as also suggested by other researchers.

FTIR has become an important tool in understanding the involvement of functional groups in relation between metal particles and biomolecules. It is used to search the chemical composition of the surface of the AgNPs and identify the biomolecules for capping and efficient stabilization of the metal nanoparticles. There were many functional groups present which may have been responsible for the bio-reduction of Ag^+ ions. The flavonoids present in the flower extract are powerful reducing agent which may be suggestive for the formation of silver nanoparticles by reduction of silver nitrate (Table 1). But, the probable mechanism is unclear and needs further investigation.

XRD analysis proved that silver nanoparticles were crystalline in nature. TEM analysis revealed that *T. erecta* flower AgNPs were spherical, hexagonal and irregular in shape. The shape and size of nanoparticles formed varies from plant to plant and part used and also the phytoconstituents like alkaloid, flavonoids, tannins and cardiac glycoside present in them at the time of synthesis (Table 1).

AgNPs from *Annona squamosa* leaf extract were spherical in shape with an average size ranging from 20 to 100 nm (Vivek et al., 2012) while Thirunavokkarasu et al. (2013) reported spherical nanoparticles with size ranging from 8 to 90 nm in *Desmodium gangeticum*. The sharp signal peak of silver strongly indicated the reduction of silver ion by *T. erecta* into elemental silver. Metallic silver nanoparticles generally show typical optical absorption peak approximately at 2.6 keV due to surface plasmon resonance. There were spectral signals for C and Cu because of the TEM grid used. From EDX spectrum, it was clear that *T. erecta* had percent yield of 71.31% of AgNPs and synthesized nanoparticles were composed of high purity AgNPs. TEM images showed that the surfaces of the AgNPs were surrounded by a black thin layer of some material which might be due to the capping organic constituents of flower broth as also reported by Rafiuddin (2013).

The results of the present work clearly showed that antibacterial activity was more when antibiotics plus AgNPs were used than when antibiotics plus acetone extract was used, as evidenced by increase in fold area. The AgNPs successfully inhibited Gram negative bacteria, even better than acetone

extract. Thakur et al. (2013) and Niraimathi et al. (2013) also reported antibacterial activity of AgNPs. The AgNPs plus antibiotics could successfully inhibit the fungal strains under investigation while acetone extract plus antibiotics could not. Antifungal activity of AgNPs with commercial antibiotics is also reported (Kim et al., 2009; Gajbhiye et al., 2009). However, they have reported against only fungi and only with 2 antibiotics i.e. fluconazole and amphotericin B respectively. The mechanism of inhibitory effects of silver ions on microorganisms is somewhat known. Some studies have reported that positive charge on the silver ion is significant for its antimicrobial activity through the electrostatic attraction between negative charge on cell membrane of microorganism and positive charged nanoparticles (Hamouda and Baker, 2000; Dibrov et al., 2002; Chanda, 2014).

Over all, it can be concluded that antibiotics plus AgNPs showed more inhibitory activity than antibiotics alone and antibiotics plus acetone extract. The inhibition was more against pathogenic fungal strains and Gram negative bacteria. This is very interesting because they both are very resistant pathogenic microbial strains causing incurable infectious diseases and there is always a look out for alternative novel approach to treat them.

To date, synthesis of AgNPs with flower extracts is scanty and synthesis of AgNPs with *T. erecta* flower extract is reported for the first time. Moreover, combination or synergistic effect of 15 antibiotics with AgNPs against pathogenic bacteria and fungi is a new finding. The reduction of silver ions occurred due to the water-soluble phytochemicals like flavonoids, tannins, triterpenes, cardiac glycosides and alkaloids present in the flower sample of *T. erecta* (Table 1). The results clearly demonstrated that AgNPs synthesized by green route can definitely compete with commercial antibiotics used for the treatment of microbial infections and sometimes are even better. Thus, these ecofriendly silver nanoparticles can be used as an excellent antimicrobial agent against multi drug resistant pathogenic microorganisms. However, more research work especially on animal models needs to be done before they can be used as antimicrobial agents. Finally the therapeutic use of nanoparticles synthesized from flowers, otherwise thrown away as useless material into environment is noteworthy.

Acknowledgements

The authors thank Prof. S.P. Singh, Head, Department of Biosciences, Saurashtra University, Rajkot, Gujarat, India for providing excellent research facilities. We acknowledge the support extended by Prof. Shipra Baluja, Department of Chemistry and Prof. D.G. Kuberkar, Department of Physics, Saurashtra University for FTIR and XRD analysis of the samples.

References

Ahmad, T., Wani, I.A., Manzoor, N., Ahmed, J., 2013. Biosynthesis, structural characterization and antimicrobial activity of gold and silver nanoparticles. Colloids Surf. B, Biointerfaces 107, 227–234.

Alizadeh, H., Salouti, M., Shapouri, R., 2013. Intramacrophage antimicrobial effect of silver nanoparticles against *Brucella melitensis* 16M. Sci. Iranica F 20 (3), 1035–1038.

Bar, H., Bhui, D.K., Sahoo, G.P., Sarkar, P., Pyne, S., Misra, A., 2009. Green synthesis of silver nanoparticles using seed extract of *Jatropha curcas*. Colloids Surf. A, Physicochem. Eng. Aspects 348, 212–216.

Chanda, S., 2014. Silver nanoparticles (medicinal plants mediated): a new generation of antimicrobials to combat microbial pathogens – a review. In: Mendez-Vilas, A. (Ed.), Microbial Pathogens and Strategies for Combating Them: Science Technology and Education. FORMATEX Research Center, Badajoz, Spain, pp. 1314–1323.

Chen, W., Cai, W., Zhang, L., Wang, G., 2001. Sonochemical processes and formation of gold nanoparticles within pores of mesoporous silica. J. Colloid Interface Sci. 238, 291–295.

Dibrov, P., Dzioba, J., Gosink, K.K., Hase, C.C., 2002. Chemiosmotic mechanism of antimicrobial activity of Ag(+) in *Vibrio cholera*. Antimicrob. Agents Chemother. 46, 2668–2670.

Frattini, A., Pellegri, N., Nicastro, D., Sanctis, O., 2005. Preparation of amine coated silver nanoparticles using triethylenetetramine. Mater. Chem. Phys. 94, 148–152.

Gajbhiye, M., Kesharwani, J., Ingle, A., Gade, A., Rai, M., 2009. Fungus-mediated synthesis of silver nanoparticles and their activity against pathogenic fungi in combination with fluconazole. Nanomed. NBM 5, 382–386.

Gengan, R.M., Anand, k., Phulukdaree, A., Chuturgoon, A., 2013. A549 lung cell line activity of biosynthesized silver nanoparticles using *Albizia adianthifolia* leaf. Colloids Surf. B, Biointerfaces 105, 87–91.

Ghani, A., 2003. Medicinal Plants of Bangladesh: Chemical Constituents and Uses. Asiatic Society of Bangladesh, Dhaka.

Henglein, A., 1993. Physicochemical properties of small metal particles in solution: microelectrode' reactions, chemisorption, composite metal particles, and the atom-to-metal transition. J. Phys. Chem. B 97, 5457–5471.

Hamouda, T., Baker, J.R., 2000. Antimicrobial mechanism of action of surfactant lipid preparations in enteric Gram-negative *bacilli*. J. Appl. Microbiol. 89, 397–403.

Jain, P.K., Huang, X., El-Sayed, I.H., EL-Sayed, M.A., 2008. Noble metals on the nanoscale: optical and photothermal properties and some applications in imaging, sensing, biology, and medicine. Acc. Chem. Res. 41, 1578–1586.

Khaydarov, R.A., Khaydarov, R.R., Gapurova, O., Estrin, Y., Scheper, T., 2009. Electrochemical method for the synthesis of silver nanoparticles. J. Nanopart. Res. 11, 1193–1200.

Kim, K.J., Sung, W.S., Suh, B.K., Moon, S.K., Choi, J.S., Kim, J.G., Lee, D.G., 2009. Antifungal activity and mode of action of silver nano-particles on *Candida albicans*. Biometals 9 (22), 235–242.

Kirtikar, K.R., Basu, B.D., 1994. Indian Medicinal Plants. Lalit Mohan Basu, Allahabad.

Kotakadi, V.S., Gaddam, S.A., Rao, Y.S., Prasad, T.N.V.K.V., Reddy, A.V., Gopal, D.V.R.S., 2014. Biofabrication of silver nanoparticles using *Andrographis paniculata*. Eur. J. Med. Chem. 73, 135–140.

Krishnamurthy, N.B., Nagaraj, B., Malaka, B.L., Liny, L., Dinesh, R., 2012. Green synthesis of gold nanoparticles using *Tagetes erecta* L. (marigold) flower extract and evaluation of their antimicrobial activities. Int. J. Pharm. Biosci. 3 (1), 212–221.

Lee, K.S., El-Sayed, M.A., 2006. Gold and silver nanoparticles in sensing and imaging: sensitivity of plasmon response to size, shape, and metal composition. J. Phys. Chem. B 110, 19220–19225.

Li, X., Wang, J., Zhang, Y., Li, M., Liu, J., 2010. Surfactant less synthesis and the surface-enhanced Raman spectra and catalytic activity of differently shaped silver nanomaterials. Eur. J. Inorg. Chem. 12, 1806–1812.

Manjunath, B.L., 1969. The Wealth of India, Raq Material. CSIR, New Delhi.

Nair, L.S., Laurencin, C.T., 2007. Silver nanoparticles: synthesis and therapeutic applications. J. Biomed. Nanotechnol. 3, 301–316.

Niraimathi, K.L., Sudha, V., Lavanya, R., Brindha, P., 2013. Biosynthesis of silver nanoparticles using *Alternanthera sessilis* (Linn.) extract and their antimicrobial, antioxidant activities. Colloids Surf. B, Biointerfaces 102, 288–291.

Pal, S., Tak, Y.K., Song, J.M., 2007. Does the antibacterial activity of silver nanoparticles depend on the shape of the nanoparticle? A study of the Gram negative bacterium *Escherichia coli*. Appl. Environ. 73, 1712–1720.

Pant, G., Nayak, N., Prasuna, R.G., 2012. Enhancement of antidandruff activity of shampoo by biosynthesized silver nanoparticles from *Solanum trilobatum* plant leaf. Appl. Nanosci. 3, 431–439.

Parashar, U.K., Saxena, S.P., Srivastava, A., 2009. Bioinspired synthesis of silver nanoparticles. Dig. J. Nanomat. Biosynth. 4 (1), 159–166.

Parekh, J., Chanda, S., 2007. *In vitro* antibacterial activity of the crude methanol extract of *Woodfordia fruticosa* Kurz. flower (Lythraceae). Braz. J. Microbiol. 38, 204–207.

Rafiuddin, Z.Z., 2013. Bio-conjugated silver nanoparticles from *Ocimum sanctum* and role of cetyltrimethyl ammonium bromide. Colloids Surf. B, Biointerfaces 108, 90–94.

Rakholiya, K., Chanda, S., 2012. *In vitro* interaction of certain antimicrobial agents in combination with plant extracts against some pathogenic bacterial strains. Asian Pac. J. Trop. Biomed., S876–S880.

Rangnekar, A., Sarma, T.K., Singh, A.K., Deka, J., Ramesh, A., Chattopadhyay, A., 2007. Retention of enzymatic activity of alpha-amylase in the reductive synthesis of gold nanoparticles. Langmuir 23, 5700–5706.

Rawani, A., Ghosh, A., Chandra, G., 2013. Mosquito larvicidal and antimicrobial activity of synthesized nano-crystalline silver particles using leaves and green berry extract of *Solanum nigrum* L. (Solanaceae: Solanales). Acta Trop. 128, 613–622.

Roopan, S.M., Rohit, Madhumitha, G., Rahuman, A.A., Kamaraj, C., Bharathi, A., Surendra, T.V., 2013. Low-cost and eco-friendly phyto-synthesis of silver nanoparticles using *Cocos nucifera* coir extract and its larvicidal activity. Ind. Crops Prod. 43, 631–635.

Sathyavathi, R., Krishna, M.B., Rao, S.V., Saritha, R., Rao, D.N., 2010. Biosynthesis of silver nanoparticles using *Coriandrum sativum* leaf extract and their application in nonlinear optics. Adv. Sci. Lett. 3, 138–143.

Singer, J.M., 1987. Investigation of the mosquito larvicidal activity of the oil of marigolds. Diss. Abs. Int. B 47 (12), 4886.

Stevanovic, M.M., Skapin, S.D., Bracko, I., Milenkovic, M., Petkovic, J., Filipic, M., 2012. Poly (lactide-co-glycolide)/silver nanoparticles: synthesis, characterization, antimicrobial activity, cytotoxicity assessment and ROS-inducing potential. Polymer 53, 2818–2828.

Suman, T.Y., Elumalai, D., Kaleena, P.K., Rajasree, S.R.R., 2013. GC–MS analysis of bioactive components and synthesis of silver nanoparticle using *Ammannia baccifera* aerial extract and its larvicidal activity against malaria and filariasis vectors. Ind. Crops Prod. 47, 239–245.

Thakur, M., Pandey, S., Mewada, A., Shah, R., Oza, G., Sharon, M., 2013. Understanding the stability of silver nanoparticles biofabricated using *Acacia arabica* (Babool gum) and its hostile effect on microorganisms. Spectrochim. Acta, Part A, Mol. Biomol. Spectrosc. 109, 344–347.

Thirunavokkarasu, M., Balaji, U., Behera, S., Panda, P.K., Mishra, B.K., 2013. Biosynthesis of silver nanoparticles from extract of *Desmodium gangeticum* (L.) DC. and its biomedical potential. Spectrochim. Acta Part A, Mol. Biomol. Spectrsc. 116, 424–427.

Tenover, F.C., 2006. Mechanisms of antimicrobial resistance in bacteria. Am. J. Med. 119 (6 Suppl. 1), S3–S10 (discussion S62–S70).

Venkatesham, M., Ayodhya, D., Madhusudhan, A., Veera Babu, N.V., Veerabhadram, G., 2014. A novel green one-step synthesis of silver nanoparticles using chitosan: catalytic activity and antimicrobial studies. Appl. Nanosci. 4, 113–119.

Vidhu, V.K., Philip, D., 2014. Spectroscopic, microscopic and catalytic properties of silver nanoparticles synthesized using *Saraca indica* flower. Spectrochim. Acta Part A, Mol. Biomol. Spectrosc. 117, 102–108.

Vivek, R., Thangam, R., Muthuchelian, K., Gunasekaran, P., Kaveri, K., Kannan, S., 2012. Green biosynthesis of silver nanoparticles from *Annona squamosa* leaf extract and its *in vitro* cytotoxic effect on MCF-7 cells. Process Biochem. 47, 2405–2410.

Wells, C., Bertsch, W., Perich, M., 1992. Isolation of volatiles with insecticidal properties from the genes tagetes (Marigold). Chromatographia 34 (5–8), 241–248.

Wichtl, M., 1994. Herbal Drugs and Phytopharmaceuticals. Medpharm Scientific Publisher, Stuttgart, 446.

Wijnhoven, S.W.P., Peijnenburg, W.J.G.M., Herberts, C.A., Hagens, W.I., Oomen, A.G., Heugens, E.H.W., 2009. Nano-silver: a review of available data and knowledge gaps in human and environmental risk assessment. Nanotoxicology 3, 109–138.

Wong, K.K., Cheung, S.O., Huang, L., Niu, J., Tao, C., Ho, C.M., Che, C.M., Tam, P.K., 2009. Further evidence of the anti-inflammatory effects of silver nanoparticles. Chem. Med. Chem. 4, 1129–1135.

Zayed, M.F., Eisa, W.H., Shabaka, A.A., 2012. *Malva parviflora* extract assisted green synthesis of silver nanoparticles. Spectrochim. Acta Part A, Mol. Biomol. Spectrosc. 98, 423–428.